전 용 필 교수지도

석사학위 청구논문

A possible role of estrogen receptors in primordial follicle activation in 3D culture model

2024

성신여자대학교 일반대학원

생물학과

이 보 영

A possible role of estrogen receptors in primordial follicle activation in 3D culture model

Adviser: Yong-Pil Cheon, Ph.D.

Submitted in partical fulfillment
of the requirements for the degree of master.

Jun, 2024

Department of Biology

The Graduate School of Sungshin University

Bo Young Lee

This is certify that we have examined the

Master's Thesis of

Bo Young Lee

Submitted to Department of Biology

Approved as to style and content

Thesis Advisor .....

Committee Chairman .....

Committee Member .....

Committee Member .....

The Graduate School of Sungshin University

ABSTRACT

A possible role of estrogen receptors in primordial follicle activation in 3D culture model

Bo Young Lee
Department of Biology
Graduate School
Sungshin University

Increased primordial follicle activation induces immoderate depletion of ovarian reserve, premature ovarian insufficiency and first step for recruiting of growing follicle pools, so the regulation of primordial follicle activation is one of the crucial steps. Steroid hormones, especially estrogen, are known to play an important role in nest breakdown and subsequent follicle development. Although a relationship between the primordial follicle activation and E_2 concentration is predicted in many studies, it is not well evaluated for dormancy or activation of primordial follicles. In this study, the anti-Müllerian hormone (*Amh*) knockout mice and in vitro culture model were employed to treat specific agonists and antagonists of the estrogen receptors and to compare the degree

of activation. ESR1 and ESR2 were colocalized in oocyte cytoplasm in dormant and active follicle. The expression levels of the *Esr1* mRNA and protein were significantly low in *Amh* KO ovary but not *Esr2* and *Gper1*. Expectedly, the ratio of phosphate mTOR and Akt1 was high in the ovary of *Amh* null mice. Interestingly in wild type ovary, MPP, estrogen receptor alpha antagonist, treated group showed the highest degree of primordial activation and the dormant follicles were high in the PPT, estrogen receptor alpha agonist treated group. In *Amh* knockout ovary, MPP and PPT did not affect and instead G-1, GPR30 agonist, blocked activation. Based on the results, it is suggested that AMH may involved in E2 mediates estrogen receptor alpha to inhibit primordial follicle activation. And in the absence of AMH, estrogen receptor alpha does not function properly, GPR30 may work instead of it. Based on the results, it is suggest that Esr1 may have roles in follicle dormancy.

CONTENTS

List of Tables

List of Figures

INTRODUCTION

Primordial police pool means ovarian reserve available to women during the reproductive life span. Increased primordial follicle activation induces immoderate depletion of ovarian reserve and premature ovarian insufficiency, so it can be the result of infertility. On the other hand, the activation group of primordial follicles is pivotal in further recruitment and selection. Because of that, the process of primordial follicle activation is critical to study the regulation of folliculogenesis first step.

In mouse ovary, after the migration of primordial germ cells to the genital ridge, oogonia produces germ cell cysts due to incomplete cytokinesis at 10.5 dpc. At 13.5 dpc, there is the transition from mitosis to meiosis to become oocytes and they are arrested at the diplotene stage of the first meiotic prophase (MI) (Jessica et al, 2021). At 17.5 dpc, apoptosis of oocyte and nest breakdown lead oocyte of early ovarian development. Pregranulosa cells invade the nests and enclose the oocyte to form individual primordial follicles. The majority of primordial follicle formation occurs within the postnatal day 3 (Lei et al, 2010).

The phosphatidylinositol 3 kinase (PI3K)/phosphatase and tensin homolog deleted on chromosome 10 (PTEN) signaling is the main pathway in primordial follicle activation (Zhao et al, 2021). In dormant follicles, PTEN converts phosphatidylinositol 4,5-bisphosphate (PIP2) into phosphatidylinositol 3,4,5-trisphosphate (PIP3) to suppress the activation. In the activated follicle, the PI3K/PTEN signaling pathway is activated, PIP2 is converted to PIP3. And phosphatidylinositol-dependent kinase1 (PDK1) and AKT recruited by PIP3 are

phosphorylated and activated. Then AKT phosphorylates Foxo3 which is exported from the nucleus to the cytoplasm as a result of activation. Additionally, rapamycin complex 1 (mTORC1) pathway initiates primordial follicle activation in pregranulosa cells by activating PI3K/AKT signaling. In dormant follicles, the number of KIT ligands which is expressed by pregranulosa cells is too small to activate the KIT in oocytes. In the growing follicle, activated mTORC1 signaling induces the increased expression of KITL, leading to the phosphorylation of KIT Y719 and activation of PI3K signaling in oocytes (Kui et al, 2009).

Estrogen plays an important role as a feedback regulator of gonadotrophin secretion and intrafollicular modulator (Hisaw,1947). In previous study, E2 level in maternal and neonatal mice is higher at birth and dropped within postnatal day 3, then began to increase from day 4. A high E2 level inhibits nest breakdown and oocyte apoptosis before birth, and the level is lowered to coincide with the time when the primordial follicle is formed. (Lei Le et al, 2010). Not only estrogen, phytoestrogen, genistein treatment inhibits nest breakdown and primordial follicle assembly but have no effect on oocyte number both in organ culture and in vivo (Pepling et al, 2007). So in nature, the drop of estrogen at birth causes the oocyte nest to disassemble into single oocytes. The mouse ovaries that were cultured in high E2 medium first and in low E2 plus FSH from day 4 showed the proper primordial folliculogenesis and the highest expression of oocyte-specific gene, Figla, Nobox. Thus the changing timing of medium that contains different hormone levels is also important in in-vitro culture (Lei et al, 2010) and there may be a critical relationship between the primordial follicle activation and E2 concentration in ovary.

Additionally, estrogen can activate various intracellular events via nuclear

estrogen receptors, ER alpha and beta, and the membrane estrogen receptor, G protein-coupled receptor (GPR30). Estrogen enters the plasma membrane and binds to ER alpha and beta. Then the complex dimerizes and translocates to the nucleus to induce transcriptional changes the target genes. They bind to the estrogen response elements (EREs) that are close to the promotor or within enhancer regions. Several genes that do not include ERE sequences, estrogen receptors can interact with other transcription factors to regulate genes indirectly (Fuentes et al, 2019). And membrane-bound ER mediates nongenomic signaling of estrogen. It regulates cytoplasmic events such as protein kinase cascades and cAMP second messenger cascades to effect indirect changes of gene expression (Albanito, 2007). Several studies reported that Tamoxifen, a selective estrogen receptor antagonist, promoted primordial follicle activation and modified the ECM around follicles in the mouse ovary (Wei et al, 2022). And MPP, ESR1 specific antagonist, fully blocked estrogen effect on oocyte cyst breakdown and primordial follicle assembly (Pepling, 2009). There was a study that *Esr2* null mice and ESR2 selective antagonist PHTPP treated wild type mice resulted in increased activation of primordial follicles. And oocyte-derived factors as well as upstream regulators of AKT signaling were upregulated in *Esr2* null ovaries (Chakravarthi et al, 2020). Therefore, it is expected that there may be a critical relationship between the primordial follicle activation and E2 concentration in ovary. So we wondered to know which estrogen receptors had the most significant effect on this primordial follicle activation process.

Anti-Müllerian hormone (AMH) is a member of TGF-β family and plays a pivotal role in early folliculogenesis. AMH regulates the rate of primordial follicles entering the growing pool, so it inhibits the development of primordial

follicles (Themmen et al, 2002). AMH null mouse showed that more primordial follicles are recruited than wild type and depletion of primordial follicles at an earlier age (Themmen et al, 1999). Therefore, it is used as a potent subject for ovarian reservation.

So here, the possible role of estrogen receptors in primordial follicle activation was studied in *in vitro* culture model with *Amh* knockout mice. This experiment identifies the localization of estrogen receptors according to whether it is a dormant follicle or an activated follicle. In comparison with *Amh* knockout mice, the changes in the expression of key factors in the activation process were measured. During *in vitro* culture, ER agonist and antagonist were employed to evaluate the possible roles of ER. In addition, the relations between ERs and AMH were evaluated.

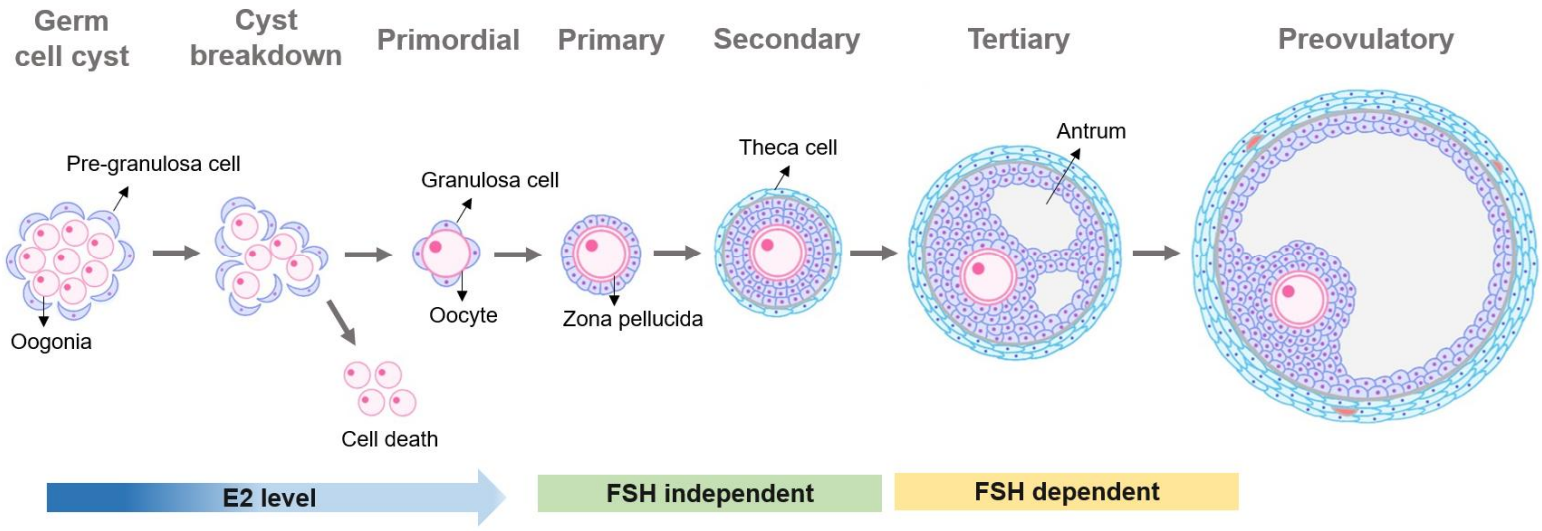

Figure 1. Diagram of folliculogenesis

The oocyte goes through a process called folliculogenesis until ovulation. In the fetal mouse ovary, primordial germ cells undergo mitotic division between 10 and 12.5dpc and oogonia forms germ cell cyst with pre-granulosa cells. Invasion of pregranulosa cells in the cyst occurs cyst breakdown, and the majority of the oocytes become apoptosis. Then the oocytes surrounded by granulosa cells form primordial follicles. After this process, follicular stages were defined as primordial follicles (follicles with single layer of flattened granulosa cells surrounding an oocyte), primary

follicles (follicles with single layer of cuboidal granulosa cells), secondary follicles (follicles with two or more layers of cuboidal granulosa cells), tertiary follicles (follicles where a cavity in the granulosa cells appear or antrum formation begins), preovulatory follicles (follicles with large antrum).

MATERIALS AND METHODS

Experimental animals

All experimental animals were conducted according to the Guide for the Care and Use of Laboratory Animals published by the National Institute of Health (NIH). All experiments were approved by the Institutional Animal Care Use Committee (IACUC) in Sungshin Women's University (SSWIACUC-2021-002). 6-8-weeks-old C57BL/6, heterozygous and homozygous B6;129S7-AMH$^{tm1Bhr/J}$ female mice were maintained under the light-on at 6:00 am and light-off at 7:00 pm, and clean room system. Animals were fed a standard rodent diet and water ad libitum from weaning at 28 days after birth.

Total RNA extraction and cDNA synthesis

Total RNA was extracted using RNeasy micro kit (Qiagen, #74004, Germany). Briefly, reaction reagents are 34 μl total RNA, 10 μl MMLV 5X buffer, 1 μl oligo dT primer (0.5 μg/μl), 1 μl random primer (0.1 μg/μl), 2 μl dNTP mix (100 mM). Reaction mixture was incubated at 65℃ for 5 min, placed the tube at RT for 5 min, and then added 4.5 μl DTT (100 mM), 2 μl M-MLV Reverse Transcriptase (Promega, #M170B, Wisconsin, USA), 1 μl RNase block ribonuclease inhibitor (40 U/ml). The mixture was incubated at 42℃ for 1 hr and 70℃ for 15 min to terminate cDNA synthesis. And kept -20℃ before it used.

Real-time PCR analysis

For quantification of expression levels, transcripts of target genes were

amplified using reverse transcript (RT)-PCR and the specific primers (Table 2). Quantification real time RT-PCR was performed using SYBR Premix Ex Taq™ (TaKaRa, #RR420, Shiga, Japan) and AriaMx Real-time PCR System (Agilent, #G8830A, California, USA). Information of the thermal cycle are in Table 1. Each reaction was run in triplicate and consisted of 1 μl cDNA. Dissociation curves were run on all reactions to ensure amplification of a single product with the appropriate melting temperature. The fold change in gene expression was calculated using the ΔΔCt method with the housekeeping gene, ribosomal protein, *36B4*, as the internal control.

Protein extraction and Western blotting analysis

Ovaries were homogenized in cold homogenization buffer (50 mM Tris-Cl, 150 mM NaCl, 10 mM β-mercaptoethanol, 2 mM $CaCl_2$, 0.1 mM PMSF, 1μM Leupeptin, 1 μM Pepstatin, 0.5 mM EDTA, 15% Glycerol, and 0.1% NP-40). The homogenates were centrifuged to remove insoluble materials. The protein concentration was determined by BCA assay (Thermo Fisher Scientific, #23225, Massachusetts, USA). 20 μg /ml of protein were boiled in SDS/β-mercaptoethanol sample buffer, and loaded onto 10% SDS-PAGE. The proteins were separated by electrophoresis and then electrotransferred onto polyvinylidene difluoride (PVDF) membranes (Bio-Rad, #1620177, California, USA) in transfer buffer (25 mM Tris base, 192 mM Glycine, 0.1% SDS, and 20% Methanol). The membranes were blocked in 10% skimmed dry milk in TBST buffer (10 mM Tris-HCl, 150 mM NaCl and 0.05% Tween-20) for 1 hr at RT, and washed three times with TBST. The membranes were incubated during overnight with 1st antibody (Table 3) at 4℃. After incubation, membranes were washed

three times and incubated for 1 hr with horseradish peroxidase-conjugated goat anti-rabbit IgG (dilution 1:2000); goat anti-mouse IgG-HRP (dilution 1:2000) for 1 hr. The bands were detected using ECL solution (Bio-Rad, #1705060, California, USA) by ChemiDoc MP Imaging System (Bio-Rad, #17001402, California, USA). The intensity of each band was normalized with total protein using ImageJ software.

In vitro culture

Ovaries were collected at PND1 and placed into cultured for 7 days. After 1% agar is hardened thinly on 4-well culture plates, medium adaptation was performed twice for 1 hour using 1ml DMEM-Ham's F-12 media (Sigma, #D2906, Burlington, USA) supplemented with 0.1% BSA (BOVOGEN, #BSA100, Melbourne, Australia), 0.1% Albumax (gibco, #2555667, Burlington, USA), 0.05mg/ml L-ascorbic acid (Sigma, #A4403, Burlington, USA) and ITS (Sigma, #I3146, Burlington, USA). Ovaries were cultured in control medium alone or the presence of estrogen receptor agonists or antagonists. Information of the chemicals is presented in Table 4. All the chemicals were dissolved in DMSO at each stock concentration and then treated to control media to final concentration. The medium under culture was collected by changing at the same time each day.

Ovarian follicle counting

Ovaries were fixed in 4% paraformaldehyde with picric acid at 4℃. The 1 hr-fixed ovaries were dehydrated in alcohol series, and embedded in paraffin using Leica EG1150H. The paraffin block was serial-sectioned at 3 μm using Leica RM2245 microtome and every 10th sections were stained with hematoxylin and

eosin Y. Tissue were microphotographed using Leica Labovert microscope and Nikon digital sight DS-Fi1 microscope digital camera. Follicles were identified as normal if they contained an intact oocyte, organized granulosa and thecal cell layers, and no pyknotic bodies. Adopting the following classification, follicular stages were defined as (1) primordial follicles: follicles with one layer of flattened granulosa cells surrounding an oocyte, (2) Primary follicles: follicles with one layer of cuboidal granulosa cells, (3) Secondary follicles: follicles with two or more layers of cuboidal granulosa cells, (4) Tertiary follicles: follicles where a cavity in the granulosa cells appear and/or antrum formation begins, (5) Preovulatory follicles: follicles with large antrum (Fig. 1).

Immunofluorescence

3 μm sections were mounted on glass slides and subjected to antigen retrieval in boiling 10mM sodium citrate buffer (pH 6.0) for 12 min. Tissues were incubated with 1% normal goat-blocking serum in PBS for 2 hr. Briefly, tissues were incubated with 1% normal goat-blocking serum in 0.1% BSA in PBS for 1 hr. And then samples were incubated with rabbit monoclonal Estrogen receptor alpha antibody (dilution 1:300), rabbit polyclonal Estrogen receptor beta antibody (dilution 1:300), and rabbit polyclonal GPR30 antibody (dilution 1:300) in a blocking solution for 2 hr. Tissues were washed with PBS. Then tissues were incubated with anti-rabbit IgG conjugated Alexa Fluor 488 (dilution 1:500, Cell signaling, #4412, Massachusetts, USA) for 1 hr. After washing it with PBS, tissues were incubated with mouse monoclonal FOXO3A antibody (dilution 1:300) 2 hr. Then tissues were incubated with anti-mouse IgG conjugated Alexa Fluor 594 (dilution 1:500, Cell signaling #8890, Massachusetts, USA) for 1 hr. Tissues were

washed and incubated with DAPI staining solution (dilution 1:1000) for 30 min. Lastly, tissues were washed and mounted with Fluoromount Aqueous mounting medium (Sigma, #F4680, Burlington, USA). Fluorescence signal was imaged on LSM700 confocal microscope (Carl Zeiss).

RNA-seq profiles acquisition

Raw data was downloaded from NCBI GEO (http://www.ncbi.nlm.nih.gov/geo). The GSE179888 datasets include bulk RNA-seq for the whole mouse ovary at specific time points. Total RNA was isolated and sequenced using an illumina high seq 2500. Raw data was analyzed using TopHat. The process of analysis was performed using the Gene set enrichment analysis (http://www. gsea-msigdb.org).

ELISA

Culture medium was collected during the culture time. 17β-estradiol, progesterone, and testosterone concentration were measured using ELISA kit (Enzo Life Sciences, #ADI-900-008, #ADI-900-011, #ADI-900-065, New York, USA), in accordance with the manufacturer's instructions. The absorbance of light was determined with a microplate reader (SpectraMax M5/M5, California, USA).

Statistics

All experiments were conducted at least in triplicate. The Student's t-test, one-way ANOVA and Tukey's multiple-comparison test was performed to evaluate the statistical significance between control and experiment group. Results were

presented as mean ± standard errors of the means (SEM). Values of $P < 0.05$ were considered to be significantly different. All analyses were done using IBM SPSS statistic.

Table 1. Real-time RT-PCR Thermal cycler schedule

Step		Temperature (℃)	Time	cycles
Hold		94	30 min	1
3 steps PCR	Denaturation	95	1 min	45
	Annealing	59	30 sec	
	Extension	72	1 min	
Dissociation	Denaturation	95	15 sec	1
	Annealing	60	30 sec	
	Extension	95	15 sec	
Hold		4	Indefinitely	1

Table 2. Primer sequences for quantitative real-time PCR

Gene	Symbol	NCBI gene reference		Primer sequence (5'-3')	Amplified length (bp)
estrogen receptor 1 (alpha)	***Esr1***	NM_001302531.2	S	CTGTGCCGTGTGCAATGACTAT	249
			AS	TGCTTCAACATTCTCCCTCCTC	
estrogen receptor 2 (beta)	***Esr2***	NM_010157.3	S	CCAGACTGCAAGCCCAAATGT	219
			AS	CTCTTGGCGCTTGGACTAGTAACA	
G protein-coupled estrogen receptor 1	***Gper1***	NM_029771.3	S	GAAGATGACCATCCCAGACCTGTA	205
			AS	TAGGTACCTGTCGAAGCTCATCCA	
forkhead box O3	***Foxo3***	NM_001376967.1	S	TGGGCAACCAAGGAAATGCT	207
			AS	TTGTGCCGGATGGAGTTCTT	
mechanistic target of rapamycin kinase	***mTOR***	NM_020009.2	S	AATGAGGAGACCAGGGCCAAA	204
			AS	ATTCCCACCTTCCACTCCTATGAG	
thymoma viral proto-oncogene 1	***Akt1***	NM_001165894.2	S	CATGAACGACGTAGCCATTCTG	195
			AS	GTCTTCATCAGCTGGCATTGTG	
cytochrome P450, family 11, subfamily a, polypeptide 1	***Cyp11a1***	NM_001346787.1	S	CAGTATGCTGGCTAAAGGACTTTCC	215
			AS	TTTTCTGTGTGCCACTCTCCCT	
cytochrome P450, family 17, subfamily a, polypeptide 1	***Cyp17a1***	NM_007809.3	S	CAGATGGTGACTCTAGGCCTCTTGT	221
			AS	AAGATGAGCGTAGACAGATCTCGGG	
cytochrome P450, family 19, subfamily a, polypeptide 1	***Cyp19a1***	NM_001348171.1	AS	GGGCGAGATGATAAGGTTCTATCAG	225
			S	GTTCTATGGGAAGAAAGCAGTGGTG	
zona pellucida glycoprotein 3	***Zp3***	NM_011776.1	S	TCTGGAAGCTGAACTAGTGGTGACT	195
			AS	TACACCAGGGCATCTTTCGTCA	

inhibin beta-A	***Inhba***	NM_008380.2	S AS	GCTCAAGTGCCAATACCATGAAGAG AATCCTCTCAGCCAAAGCAAGG	229
growth differentiation factor 9	***Gdf9***	NM_008110.2	S AS	CAGAGTGGAGCCAGTGAAAATGTG TAGAGGTGACTTCTGCTGGGTTTG	236
synaptonemal complex protein 1	***Sycp1***	NM_011516.2	S AS	CCATGCTCGAACAGGTTGCTAA GCTTTTCCGCTGGGCTTCAAT	220
STAG3 cohesin complex component	***Stag3***	NM_016964.2	S AS	GATGTCCACTGAGACCTGAAAGGA AGTTCCCTGTGAGTCT TGTCATCA	232
REC8 meiotic recombination protein	***Rec8***	NM_001360389.1	S AS	GTGAACCCAGGAGCAAAGATGT ATCACACCAATCTGAAGCTGGG	251
ankyrin 1,	***Ank1***	NM_001110783.3	S AS	AAGAAGAAGGCCGATGCTGCTA TGTTCCCCTTCTTGGTTGTCGT	220
60S acidic ribosomal protein P0	***Rplp0 (36B4)***	NM_007475	S AS	CGACCTGGAAGTCCAACTACTTCCT GCACCTTATTGGCCAACAGCAT	303

Table 3. Antibody information

Antibody	Description	Cat #	Company
Estrogen receptor alpha	Rabbit monoclonal	Ab32063	Abcam
Estrogen receptor beta	Rabbit polyclonal	PA1-313	Invitrogen
GPR30	Rabbit polyclonal	PA5-28647	Invitrogen
mTOR	Rabbit monoclonal	#2983	Cell signaling
p-mTOR	Rabbit monoclonal	#5536	Cell signaling
AKT	Rabbit monoclonal	#4685	Cell signaling
p-AKT	Rabbit monoclonal	#4060	Cell signaling
FOXO3A	Mouse monoclonal	#66428-1	Proteintech
p-FOXO3A	Rabbit monoclonal	#9464	Cell signaling

Table 4. Chemical information

Chemical	Company	Cat #	Final concentration
PPT 4,4',4''-(4-Propyl-[1H]-pyrazole-1,3,5-triyl)trisphenol	Tocris	#1426	10^{-8} M
DPN 2,3-bis(4-Hydroxyphenyl)-propionitrile	Tocris	#1494	10^{-8} M
G-1 (±)-1-[(3aR*,4S*,9bS*)-4-(6-Bromo-1,3-benzodioxol-5-yl)-3a,4,5,9b-tetrahydro-3H-cyclopenta[c]quinolin-8-yl]- ethanone	Tocris	#3577	10^{-7} M
MPP dihydrochloride 1,3-Bis(4-hydroxyphenyl)-4-methyl-5-[4-(2-piperidinylethoxy)phenol]-1H-pyrazole dihydrochloride	Tocris	#1991	10^{-6} M
PHTPP 4-[2-Phenyl-5,7-bis(trifluoromethyl)pyrazolo[1,5-a]pyrimidin-3-yl]phenol	Tocris	#2662	10^{-7} M
G15 (3aS*,4R*,9bR*)-4-(6-Bromo-1,3-benzodioxol-5-yl)-3a,4,5,9b-3H-cyclopenta[c]quinoline	Tocris	#3678	5 μM

RESULTS

Localization of estrogen receptors in dormant and activated follicles

In fresh ovaries (postnatal day 1), changes in estrogen receptors localization according to primordial follicle activation were investigated by immunofluorescence. If a dormant follicle is activated, foxo3a which was located in the nucleus translocates to the cytoplasm. And activated follicle has a larger oocyte and granulosa cells look a cuboidal shape. Thus, to use Foxo3a as a make for primordial follicle activation marker, we costained each estrogen receptor and Foxo3a. Estrogen receptor alpha was mainly located in the cytoplasm of oocytes, which were found at the same localization in the dormant and growing follicles (Fig. 2A). Also, estrogen receptor beta was detected in the cytoplasm of oocytes in both dormant and activated follicles (Fig. 2B). GPR30 was detected in the cell membrane of all follicles (Fig. 2C). These localization patterns of estrogen receptor were similar without significant differences in wild type and *Amh* knockout (Fig. 2D, E, F). *Amh* knockout group showed a slightly more growing follicle including larger oocytes.

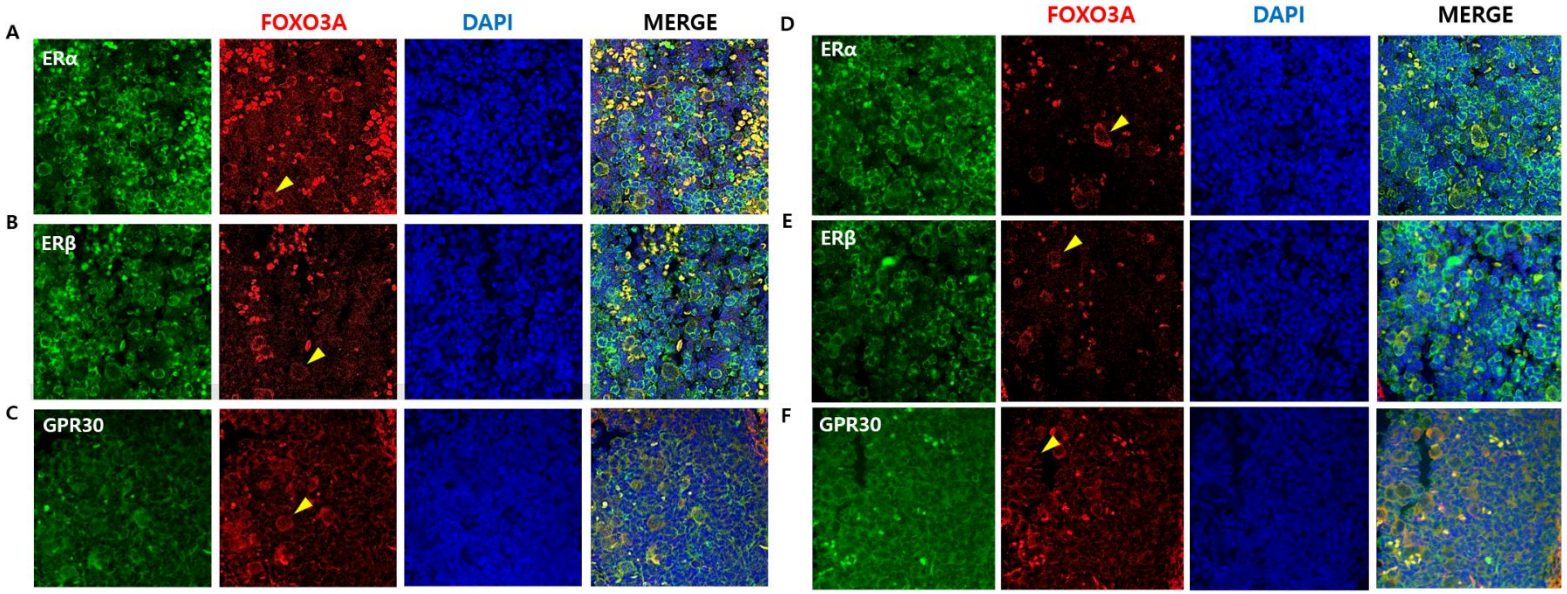
A
FOXO3A
DAPI
MERGE
ERα
B
ERβ
C
GPR30
D
FOXO3A
DAPI
MERGE
ERα
E
ERβ
F
GPR30

Figure 2. Localization of estrogen receptors in dormant and activated follicles.

Fresh ovary performed immunofluorescence staining before culture. Every slide costained with each estrogen receptor (green) and the activation marker, FOXO3A (red), and the nuclear marker, DAPI (blue). (A) ERα, (B) ERβ, and (C) GPR30 are wild type results. (D) ERα, (E) ERβ, and (F) GPR30 are *Amh* knockout results. Arrow indicated the most representative activated follicles. Magnification : X400.

Differences in expression pattern of estrogen receptors and primordial follicle activation-related genes according to genotypes in postnatal day 1

In PND1, mouse ovaries were collected and quantitative real time PCR analysis was performed to examine genotype dependent transcriptional difference before culture. Both Esr1, Esr2 and GPR30 showed decreased gene expression in the *Amh* knockout group. Only Esr1 was significantly reduced in *Amh* knockout (Fig. 3A).

In addition, mTOR plays a pivotal role in differentiation of pregranulosa cell to initiate oocyte activation. It causes dormant oocytes to awaken through KIT ligand and this network is connected to PI3K-AKT signaling. If PI3K signaling is activated, phosphorylated Akt1 by PIP2 is recruited and makes Foxo3 activated. Therefore, the transcriptional changes in the Foxo3, mTOR, Akt1 genes were also investigated. The mRNA expression of mTOR and Foxo3 also downregulated in *Amh* knockout, especially mTOR showed significant change (Fig .3D, E). Exceptionally, Akt1 showed a similar level in both groups (Fig. 3F).

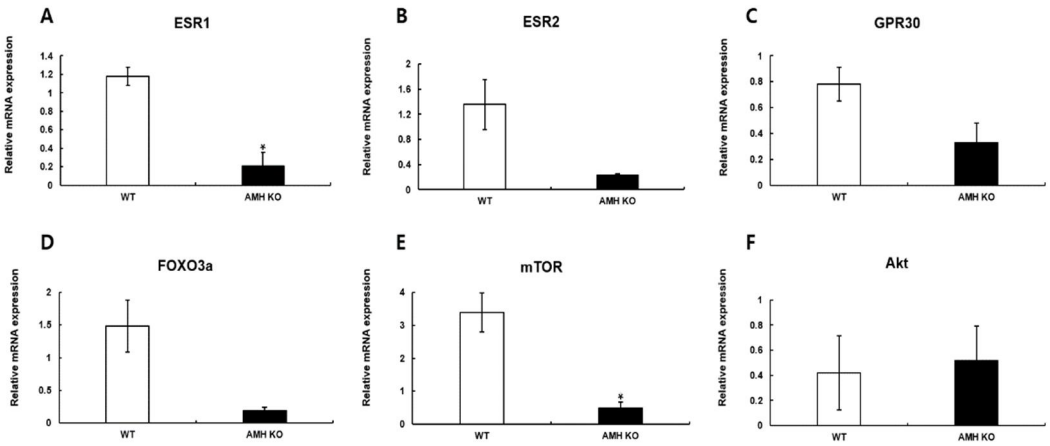

Figure 3. Transcriptional analysis of estrogen receptors and mTOR/PI3K/AKT pathway-related genes in wild type and *Amh -/-* ovaries at postnatal day 1. Gene expression was measured by RT-qPCR and compared wild type to *Amh* knockout. mRNA level was calculated using the ΔΔCt method with the *36B4*, as the internal control. *: $p < 0.05$ (wild type vs *Amh* knockout group). Data are represented as the mean ±SEM.

Protein expression profiles of estrogen receptors and primordial follicle activation-related genes according to genotypes in postnatal day 1

Following the confirmation of the mRNA level, Western blotting was performed to determine the protein expression profiles The *Amh* knockout group showed a decrease in estrogen receptors expression compared to wild type (Fig. 4F). In a similar tendency to the mRNA level, only estrogen receptor alpha protein was significantly decreased in the *Amh* knockout ovary.

In order to study whether the mTOR/PI3K/AKT signaling pathways were activated, the ratio of phosphorylated protein to total protein was investigated. We found that in *Amh* knockout ovaries, the activity of mTOR and Akt1 was significantly enhanced, as indicated by the elevated levels of phosphorylated ratio (Fig. 4G, H). These results suggest that compared to wild type, *Amh* knockout ovary could have a change in balancing the dormancy and activation of primordial follicles.

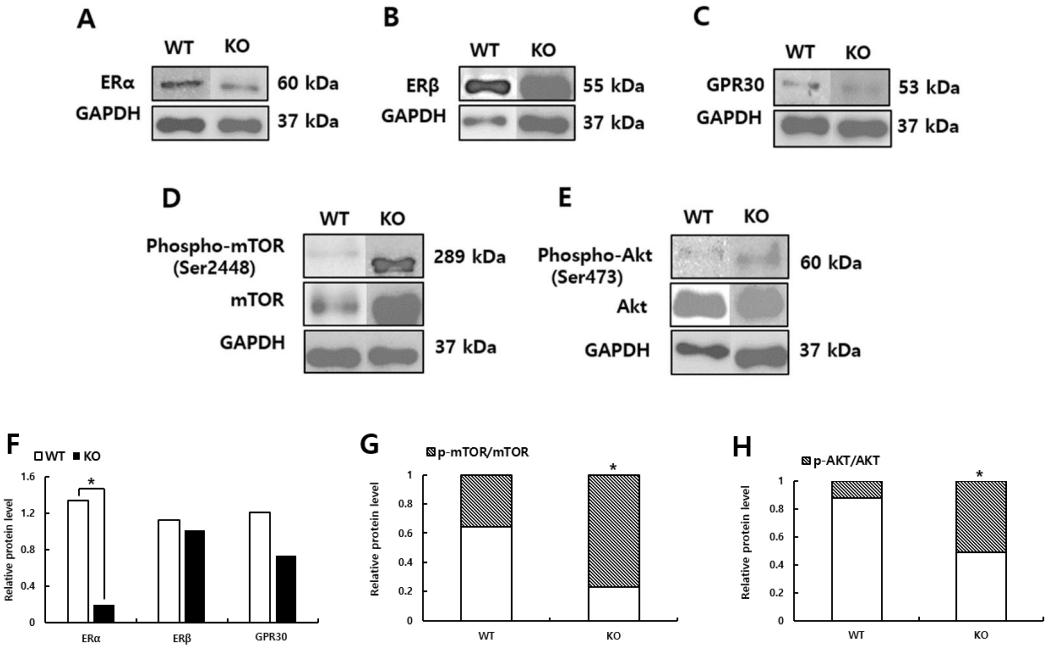

Figure 4. Protein expression profiles of estrogen receptors and mTOR/PI3K/AKT pathway-related genes in wild type and *Amh -/-* ovaries at postnatal day 1.

Western blot analysis of fresh ovary to compare wild type and *Amh* knockout group. The target protein levels were normalized to GAPDH. Intensity is measured using the ImageJ system. * : $p < 0.05$ (wild type vs *Amh* knockout group). Data are represented as the mean ±SEM.

Clustering-based analysis of GSE179888 RNA-seq data to compare *in vivo* and *in vitro* culture conditions

By analyzing the change from postnatal day 0 to day 14 under in vivo conditions, we tried to know what difference there is when in vitro culture was performed. So publicly available GSE179888 dataset was downloaded from NCBI for analysis. This dataset contains RNAseq results for postnatal day 0, 3, 7, and 14 and was repeated twice. Up-and-down-regulated gene expression was shown for each day, and clustering was performed between those showing similar expression patterns (Fig. 5A). It was divided into a total of 6 clusters, and each cluster was carried out Gene ontology enrichment analysis.

Cluster 1, the group of genes that is most strongly upregulated on postnatal day 7, is related to the steroid metabolic process, lipid localization, and hormone metabolic process (Fig. 5B). The genes in cluster 2 are upregulated on postnatal day 14 and the largest proportion of genes is included to the regulation of the immune system, including virus (Fig. 5C). Cluster 3 and 4 similarly expressed a large number of genes in categories related to synaptic organization, axonogenesis and extracellular structure organization (Fig. 5D, E). Cluster 5 which showed strong expression on postnatal day 0 was found to correspond to myeloid cell differentiation, cellular process involved in reproduction, and the meiotic cell cycle (Fig. 5F). Lastly, cluster 6 represents the genes that are particularly upregulated on postnatal day 3 and relates to the regulation of neurotransmitter, external encapsulating structure, and cell-cell adhesion via plasma-membrane adhesion molecules (Fig. 5G).

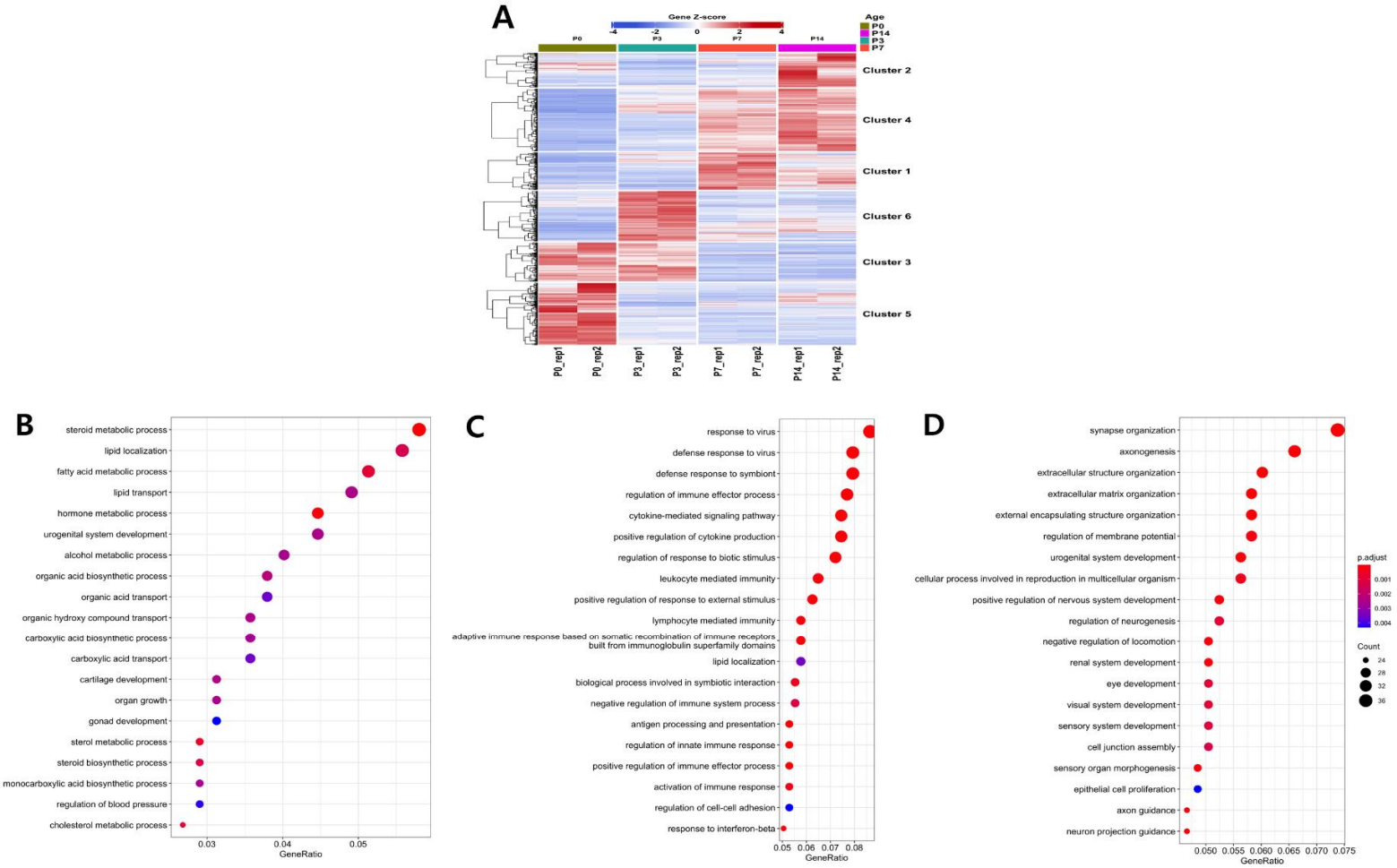
A
Gene Z-score
-4
-2
0
2
4
Age
P0
P14
P3
P7
Cluster 2
Cluster 4
Cluster 1
Cluster 6
Cluster 3
Cluster 5
P0_rep1
P0_rep2
P3_rep1
P3_rep2
P7_rep1
P7_rep2
P14_rep1
P14_rep2
B
steroid metabolic process
lipid localization
fatty acid metabolic process
lipid transport
hormone metabolic process
urogenital system development
alcohol metabolic process
organic acid biosynthetic process
organic acid transport
organic hydroxy compound transport
carboxylic acid biosynthetic process
carboxylic acid transport
cartilage development
organ growth
gonad development
sterol metabolic process
steroid biosynthetic process
monocarboxylic acid biosynthetic process
regulation of blood pressure
cholesterol metabolic process
0.03
0.04
0.05
GeneRatio
C
response to virus
defense response to virus
defense response to symbiont
regulation of immune effector process
cytokine-mediated signaling pathway
positive regulation of cytokine production
regulation of response to biotic stimulus
leukocyte mediated immunity
positive regulation of response to external stimulus
lymphocyte mediated immunity
adaptive immune response based on somatic recombination of immune receptors built from immunoglobulin superfamily domains
lipid localization
biological process involved in symbiotic interaction
negative regulation of immune system process
antigen processing and presentation
regulation of innate immune response
positive regulation of immune effector process
activation of immune response
regulation of cell-cell adhesion
response to interferon-beta
0.05
0.06
0.07
0.08
GeneRatio
D
synapse organization
axonogenesis
extracellular structure organization
extracellular matrix organization
external encapsulating structure organization
regulation of membrane potential
urogenital system development
cellular process involved in reproduction in multicellular organism
positive regulation of nervous system development
regulation of neurogenesis
negative regulation of locomotion
renal system development
eye development
visual system development
sensory system development
cell junction assembly
sensory organ morphogenesis
epithelial cell proliferation
axon guidance
neuron projection guidance
p.adjust
0.001
0.002
0.003
0.004
Count
24
28
32
36
0.050
0.055
0.060
0.065
0.070
0.075
GeneRatio

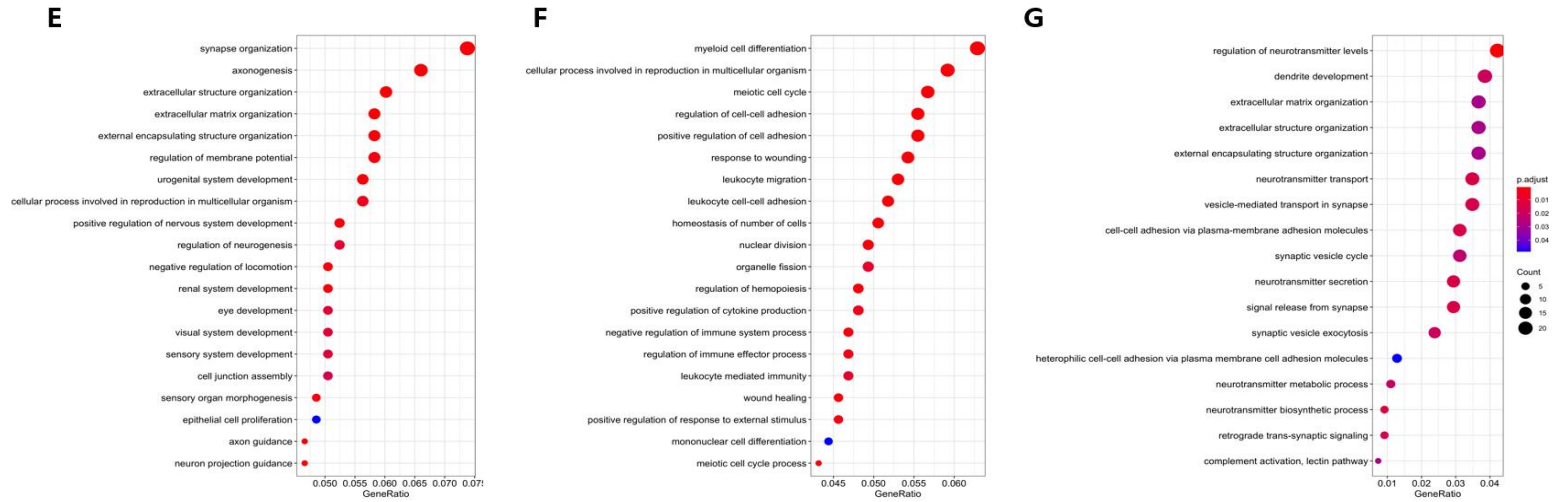

Figure 5. Clustering-based analysis of GSE179888 RNA-seq data.

(A) Clustering and heat map of GSE179888 RNA-seq data showing all the differentially expressed genes among postnatal day 0-14 samples. The samples were repeated 2 times. Red color indicates high expression and blue color indicates low expression level. The differentially expressed genes were distinguished into 6 clusters based on their expression patterns. (B) Gene ontology enrichment analysis of cluster 1. (C) Cluster 2. (D) Cluster 3. (E) Cluster 4. (F) Cluster 5. (G) Cluster 6. The size of dot represents the number of genes labeled as a GO term and the color indicates the enriched p-adjust value.

Identification of the differentially expressed genes between postnatal day 0 and day 7

In the GSE179888, postnatal day 0 and day 7 datasets were picked to compare for further study. With a cutoff of FDR<0.05, 2,927 genes were identified as significant differentially expressed genes. Of these, 1,553 genes were upregulated and 1,374 genes were downregulated in the postnatal day 7 ovaries compared to day 0 (Fig. 6A). And then, Gene Ontology enrichment analysis was performed for genes up-and down-regulated on postnatal day 7 compared to postnatal day 0. The upregulation category that contains a large proportion of genes is lipid localization, steroid metabolic process, and organic acid transport (Fig. 6B). The many genes identified in the downregulation category were related to cellular processes involved in reproduction, and meiosis (Fig. 6C).

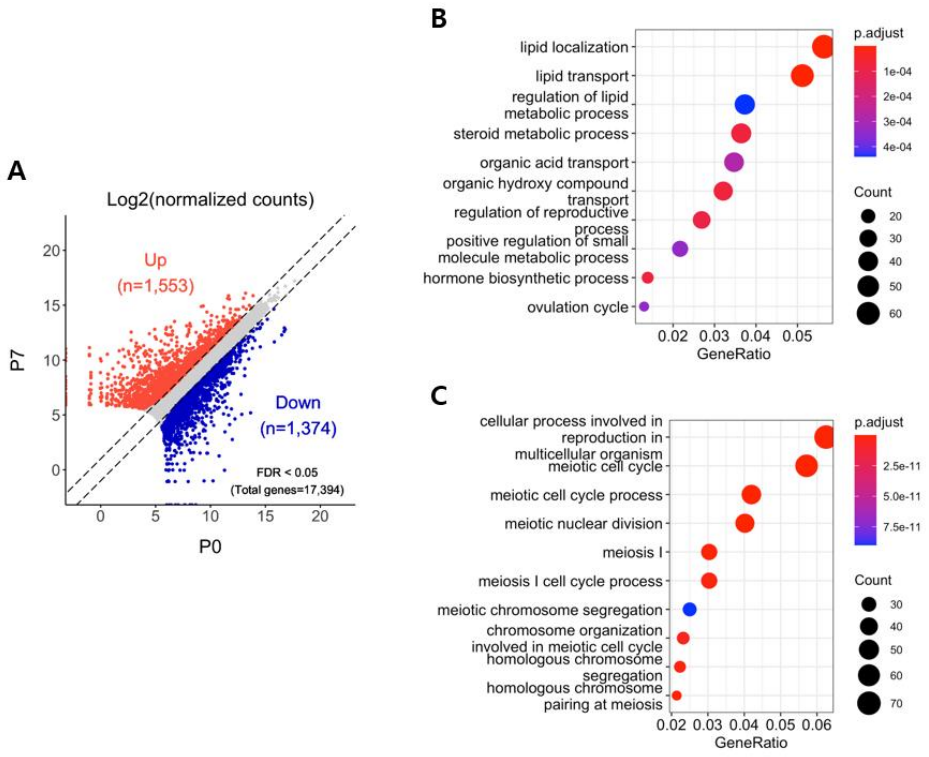

Figure 6. Scatter plot and Gene Ontology (GO) enrichment of up-and down-regulated genes.

(A) Scatter plot analysis of differentially expressed genes of postnatal day 0 and day 7 transcripts in the GSE179888. FDR < 0.05 was used as the threshold to evaluate the significance of differences in gene expression. Each red and blue dot represents up or down-regulated genes and the grey dots represent no significant genes. (B) Gene ontology enrichment analysis of up-regulated genes in postnatal day 7 compared to day 0. (C) Gene ontology enrichment analysis of down-regulated genes in postnatal day 7 compared to day 0. The size of the dot represents the number of genes labeled as a GO term and the color indicates the enriched p-adjust value.

Comparison of mRNA expression profile of genes that were up-regulated *in vivo* before and after *in vitro* culture.

Based on the analysis of RNAseq data, we tried to compare the *in vivo* data with the results of our *in vitro* culture. From the sequencing results, genes were screened from the categories upregulated at postnatal day 7 rather than postnatal day 1, similar to the time point of culture in our experiment. In gene ontology enrichment of up-regulated genes (Fig. 6B), the steroid metabolic process category and regulation of reproductive process category were selected.

First of all, Cyp11a1, Cyp17a1, and Cyp19a1 were targeted among the genes corresponding to the steroid metabolic process. These genes encode a member of the cytochrome P450 superfamily of enzymes and catalyze many reactions involved in drug metabolism and the synthesis of cholesterol, steroids, and other lipids. Cyp11a1 catalyzes the conversion of cholesterol to pregnenolone and Cyp17a1 has both 17alpha-hydroxylase and 17,20-lyase activities and then Cyp19a1 catalyzes the last steps of estrogen biosynthesis.

Next, Zp3, Gdf9, and Inhba were selected in the regulation of reproductive process category. Zp3 is a structural constituent of egg coat and is involved in the oogenesis and regulation of several gene expressions. Inhba is related endocrine regulator of the reproductive axis and regulates FSH secretion from the pituitary gland. Gdf9 is a gene known to play an important role in follicular development, and in particular, Gdf9-deficient mice have arrested in growth at the primary follicle stage. Therefore, quantitative real-time PCR analysis was performed to confirm whether the in vitro culture results showed the same increase pattern.

Similar to the in vivo sequencing results, all of the previously selected genes

increased after culture than before. This tendency was the same in the wild type and *Amh* knockout group. Especially, in wild type, Inhba showed a significant increase after culture (Fig. 7E).

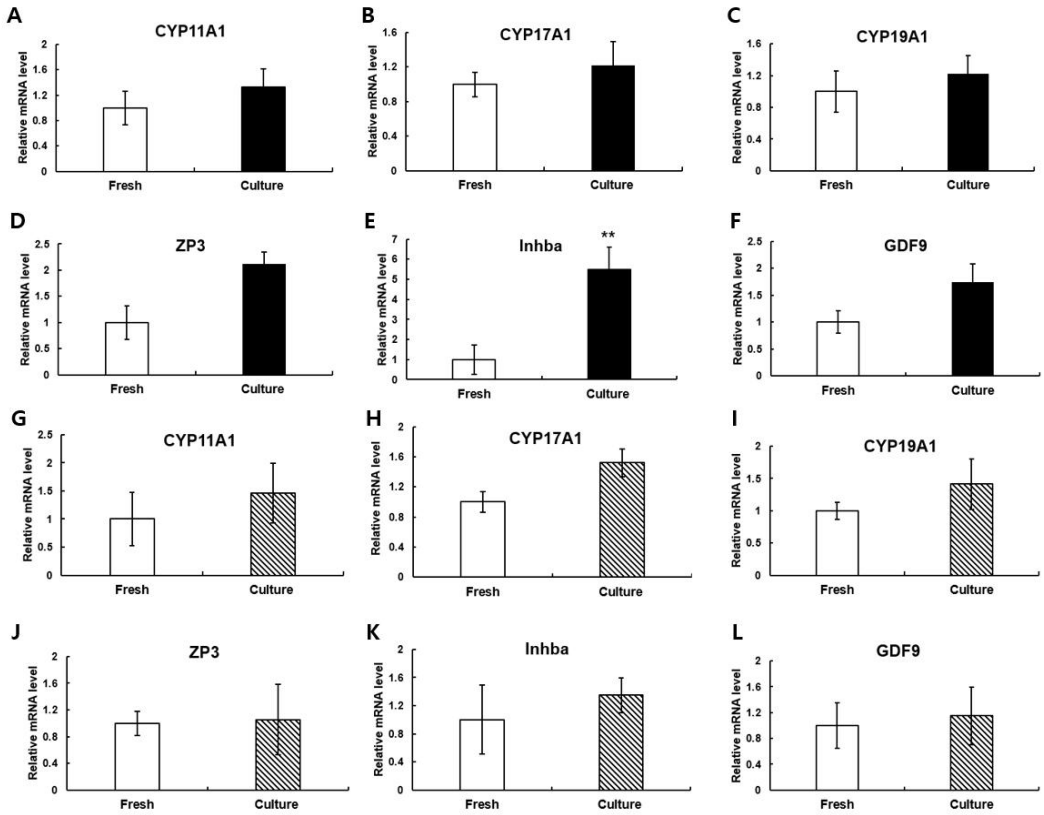

Figure 7. Transcriptional analysis of genes that were up-regulated *in vivo* before and after *in vitro* culture.

Genes were selected from the categories up-regulated rather postnatal day 7 than day 1. Gene expression was measured by RT-qPCR and compared before to after culture. (A), (B), (C), (D), (E), (F) are wild type results, and (G), (H), (I), (J), (K), (L) are *Amh* knockout group results. mRNA level was calculated using the ΔΔCt method with the *36B4*, as the internal control. *: $p < 0.05$ (Fresh ovary vs Culture group). Data are represented as the mean ±SEM.

Comparison of mRNA expression profile of genes that were down-regulated *in vivo* before and after *in vitro* culture

Furthermore, genes were screened from the categories downregulated at postnatal day 7 rather than postnatal day 1, similar to the time point of culture in our experiment. In gene ontology enrichment of down-regulated genes (Fig. 6C), meiosis Ⅰ and homeostasis category-related genes were selected.

Sycp1, Stag3, and Rec8 were chosed in meiosis Ⅰ category. There is some evidence that steroid hormones including E2 can cause a delay in meiotic progression at the diplotene stage. (Pepling et al, 2016). First, Sycp1 is a synaptonemal complex protein, so it enables double-stranded DNA binding activity. Stag3 is a subunit of the cohesion complex that regulates the cohesion of sister chromatids during cell division. When a mutation occurs in this gene, it could induce premature ovarian failure. And Rec8 localizes to the axial elements of chromosomes during meiosis in oocytes. It is a prominent component of the meiotic prophase chromosome axis that mediates sister chromatid cohesion, homologous recombination, and chromosome synapsis (Kim et al, 2016). In a previous study, all 3 genes showed downregulation of the mRNA expression when E2 was treated during the culture (He et al, 2021). Ank1 is the homeostasis-related gene. It plays a pivotal role in activities such as cell motility, activation, proliferation, and maintenance of specialized membrane domains.

Likewise, quantitative real-time PCR analysis was performed to confirm whether the in vitro culture results showed the same down-regulated pattern. Interestingly, *in vivo* sequencing results, all genes that had been downregulated showed an increase after *in vitro* culture in wild type. Notably rather the *Amh*

knockout group showed a decreasing pattern after culture, similar to the results of *in vivo.* All results showed no significant difference between culture before and after.

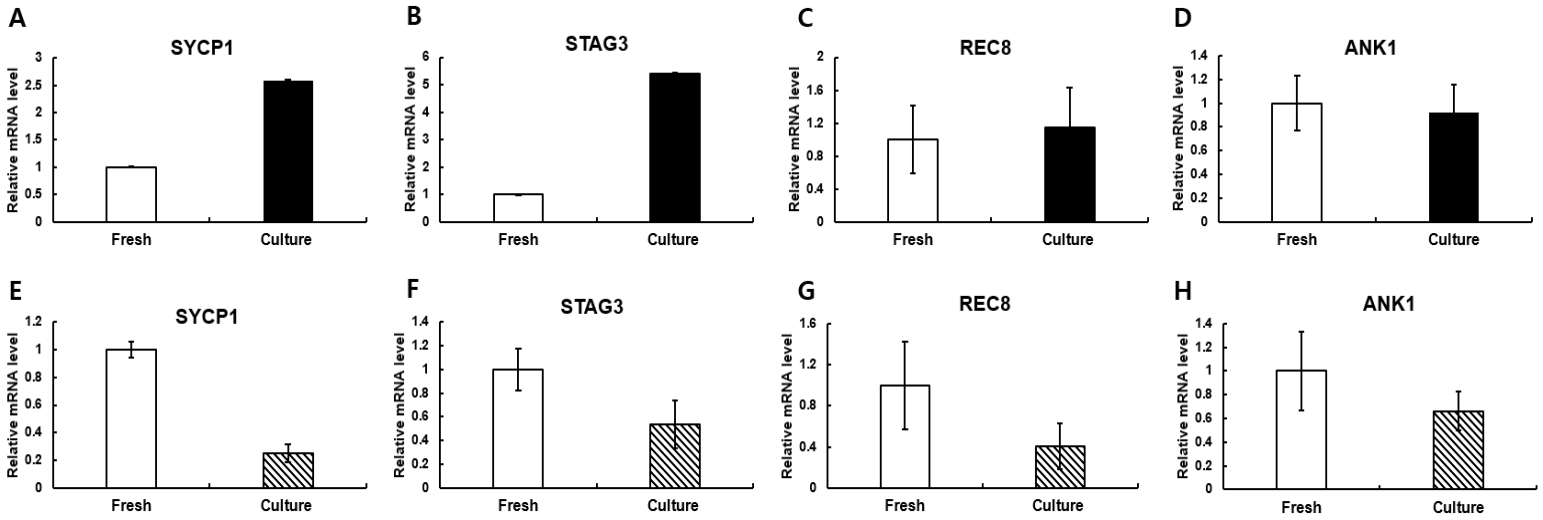

Figure 8. Transcriptional analysis of genes that were down-regulated *in vivo* before and after *in vitro* culture.

Genes were selected from the categories down-regulated rather postnatal day 7 than day 1. Gene expression was measured by RT-qPCR and compared before to after culture. (A), (B), (C), (D) are wild type results, and (E), (F), (G), (H) are *Amh* knockout group results. mRNA level was calculated using the ΔΔCt method with the *36B4*, as the internal control. *: $p < 0.05$ (Fresh ovary vs Culture group). Data are represented as the mean ±SEM.

Differences in wild type and *Amh* knockout ovaries when in vitro cultured with agonist and antagonist for estrogen receptors

To find out which estrogen receptors have the greatest influence on the process of follicle activation, ovaries were treated with each receptor's agonist and antagonist during in vitro culture for 7 days. After culture, to investigate the degree of follicle activation, the number of ovarian follicles per stage was counted.

In wild type ovary, the distribution of primordial follicles was predominant in all groups. Compared to control group, PPT, estrogen receptor alpha agonist, treated group showed the highest proportion of primordial follicles and activation seemed to be delayed. Conversely, in the case of ovaries treated with MPP, estrogen receptor alpha antagonist, displayed more than twice as many primary follicles as the control group. This group had a significantly higher activation rate (Fig. 9B). And estrogen receptor beta agonist DPN and antagonist PHTPP treated group showed a similar level of activation with control group. GPR30 agonist G-1 and antagonist G15 treated group both had fewer primary follicles than the control group. To confirm the histology results, western blotting were performed. The ratio of phosphorylated Foxo3a to total Foxo3a is used as a marker for degree of activation. Like Figure. 9P results, the degree of phosphorylation of Foxo3a was the highest in the MPP-treated group and the lowest in the PPT-treated group (Fig. 9Q).

In *Amh* knockout ovaries, since all groups had a higher proportion of entering to the growing follicle pool than wild type ovaries, it means that more activation has occurred (Fig. 10B). Similar to wild type, MPP treated group showed the most degree of activation, but it was not significant. PPT treatment group which showed the least primary follicle in the wild type was activated at just a level similar to the control group. In the DPN and PHTPP groups that regulated estrogen receptor beta,

there was no significant difference from the control group. Among them, PHTPP group had a high degree of activation, similar to MPP. G-1 treated ovary showed that the growth of primordial follicle was significantly delayed. The distribution of primordial follicles in this group was predominant, so that primary follicle is only about 10% (Fig. 10O). In western blotting result, the ratio of phosphorylated Foxo3a showed same pattern with histology experiment results.

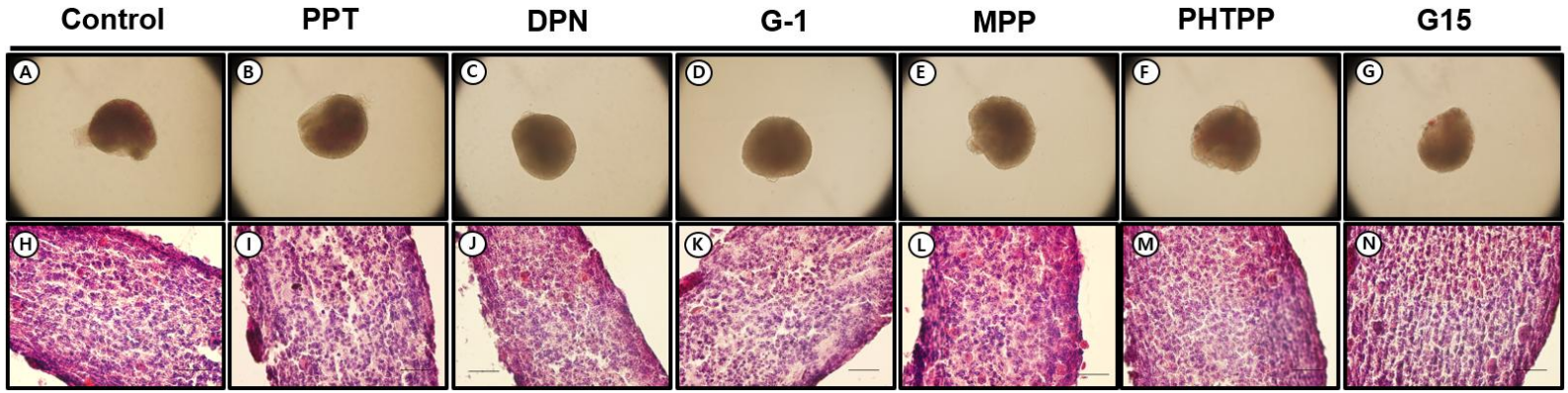
Control
PPT
DPN
G-1
MPP
PHTPP
G15
A
B
C
D
E
F
G
H
I
J
K
L
M
N

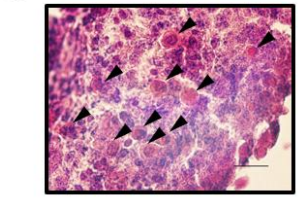
O

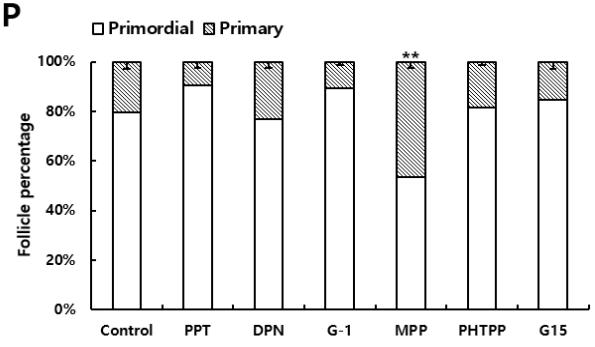
P
Primordial
Primary
100%
80%
60%
40%
20%
0%
Follicle percentage
**
Control
PPT
DPN
G-1
MPP
PHTPP
G15

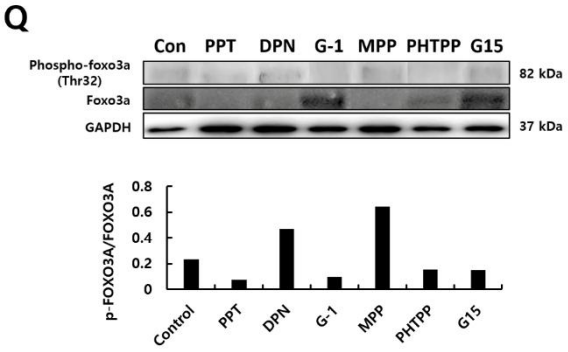
Q
Con
PPT
DPN
G-1
MPP
PHTPP
G15
Phospho-foxo3a (Thr32)
Foxo3a
GAPDH
82 kDa
37 kDa
p-FOXO3A/FOXO3A
0.8
0.6
0.4
0.2
0
Control
PPT
DPN
G-1
MPP
PHTPP
G15

Figure 9. Comparison of the number of activated follicles by culture medium in wild type ovaries.

The number of follicles was counted by H&E staining on the 5th section of the tissue sectioned to a thickness of 3μm. (A) Histological comparison of ovaries by control culture medium. (B,I) PPT. (C,J) DPN. (D,K) G-1. (E,L) MPP. (F,M) PHTPP. (G,N) G15. Magnification : X600. (O) Enlarged image of ovaries cultured in control medium. Arrow head indicates growing follicles. Magnification : X1000. (P) Comparison of follicle distribution as a percentage. (Q) Western blot analysis of cultured ovaries by culture medium. The target protein levels were normalized to GAPDH. Intensity is measured using the ImageJ system. The scale bar in the figure represents 200μm.

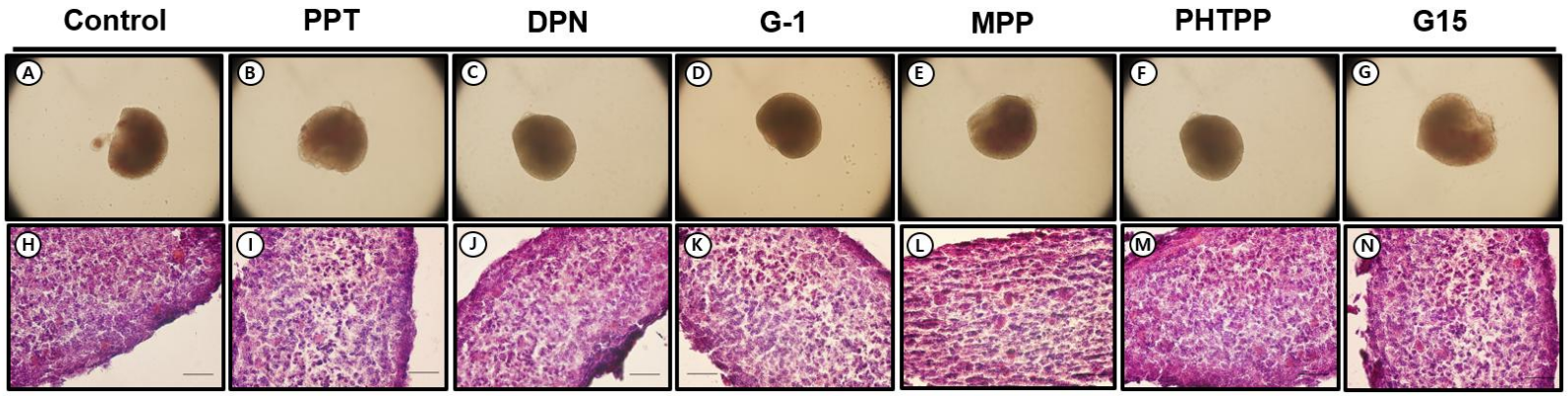
Control
PPT
DPN
G-1
MPP
PHTPP
G15
A
B
C
D
E
F
G
H
I
J
K
L
M
N

O

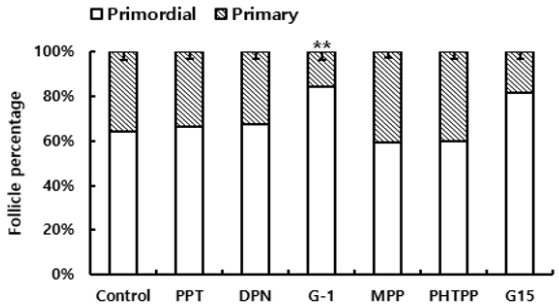
Primordial
Primary
**
100%
80%
60%
40%
20%
0%
Follicle percentage
Control
PPT
DPN
G-1
MPP
PHTPP
G15

P

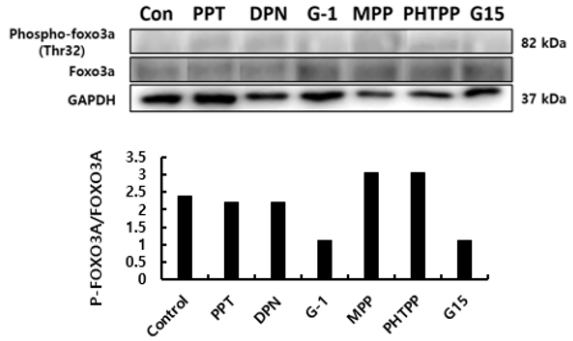
Con
PPT
DPN
G-1
MPP
PHTPP
G15
Phospho-foxo3a (Thr32)
Foxo3a
GAPDH
82 kDa
37 kDa
P-FOXO3A/FOXO3A
3.5
3
2.5
2
1.5
1
0.5
0
Control
PPT
DPN
G-1
MPP
PHTPP
G15

Figure 10. Comparison of the number of activated follicles by cultue medium in *Amh* -/- ovaries.

The number of follicles was counted by H&E staining on the 5th section of the tissue sectioned to a thickness of 3μm. (A) Histological comparison of ovaries by control culture medium. (B,I) PPT. (C,J) DPN. (D,K) G-1. (E,L) MPP. (F,M) PHTPP. (G,N) G15. Magnification : X600. (O) Comparison of follicle distribution as a percentage. (P) Western blot analysis of cultured ovaries by culture medium. The target protein levels were normalized to GAPDH. Intensity is measured using the ImageJ system. The scale bar in the figure represents 200μm.

***in vitro* culture effect by estrogen receptor ago/antagonist on the steroid hormonal level during the culture period**

During the culture period, medium was collected day by day. ELISA was performed to investigate the changes of secreted steroid hormone levels. In wild type ovaries, all three estrogen receptor agonist medium (PPT, DPN and G-1) showed a rapid increase in 17β-Estradiol levels immediately after culture and then increased again on day 6 (Fig. 11A). In the case of antagonist (MPP, PHTPP and G15), all of them had higher secretion compared to control medium, especially at G15 (Fig. 11B). The level was the highest on day 6 even at antagonist treated group. Progesterone showed a lower level than the control in PPT medium, and the level seems to increase as the culture time passed in DPN and G-1 medium (Fig. 11C). Antagonist treated group generally had more progesterone secretion than the control, and the level decreased over time contrary to agonist group (Fig. 11D). Testosterone secretion was lower than the control at PPT and G-1 medium except DPN. DPN treated group changed in a pattern similar to that of control, which was particularly reduced on day 5 (Fig. 11E). MPP treated group increased overall and then decreased sharply on day 7, and PHTPP group peaked on day 3 and subsequently decreased. And G15 medim remained at a similar level with little change (Fig. 11F).

Unlike the wild type, which showed higher 17β-Estradiol secretion compared to control in all mediums, Amh knockout ovaries showed lower secretion than control in all mediums (Fig. 12A, B). Progesterone showed that only G-1 showed a higher level than control group. PPT and DPN treated ovaries changed in a pattern similar to control. The level of G-1 increased, especially on the day 2 and 6 (Fig. 12C). In the case of antagonists, the secretion in G15 medium

increased on the day 2 like G-1, and PHTPP medium continued to increase over time. The level was maintained after decreased sharply immediately after the culture in MPP treate group (Fig. 12D). In the of testosterone, the level especially increased in G-1 medium to day 8, and the level decreased in the PPT, DPN treated group (Fig. 12E). On the other hand, in the antagonist medium, the testosterone level increased in PHTPP medium to day 8. And it also decreased in other medium (Fig. 12F).

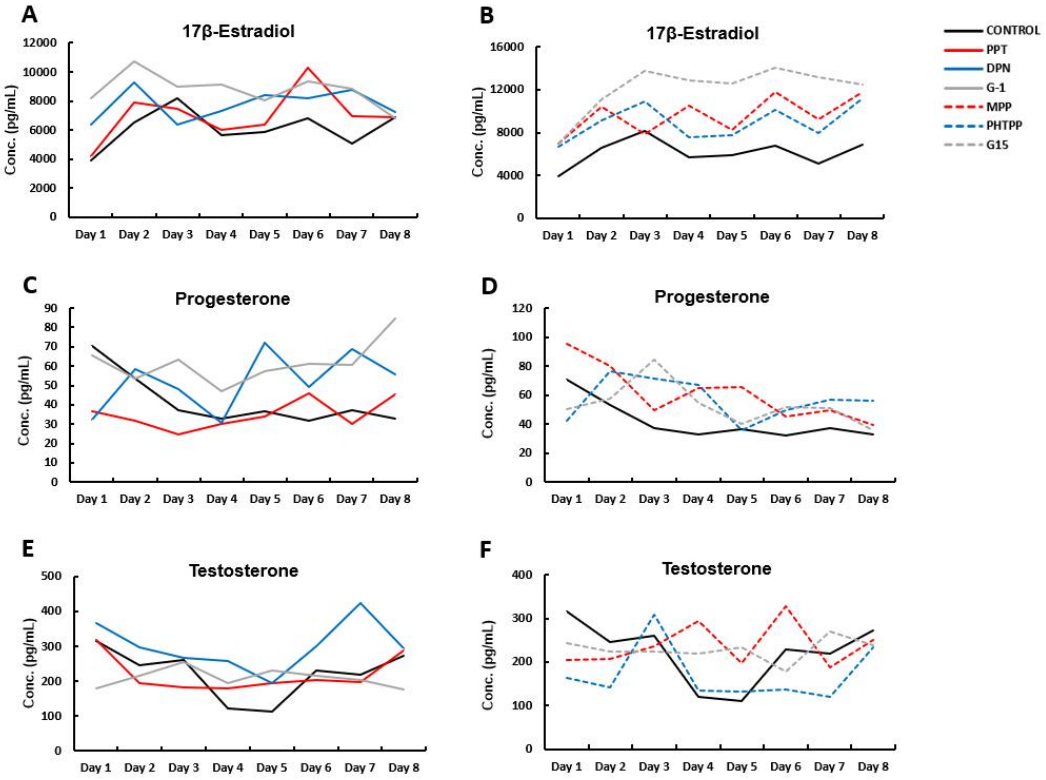

Figure 11. *in vitro* culture effect by estrogen receptor ago/antagonist on the steroid hormonal level of wild type ovaries during the culture period.

Hormonal level was estimated in spent media by the ELISA kit. (A) Level of 17β-Estradiol in ESR agonists medium. (B) Level of 17β-Estradiol in ESR antagonists medium. (C) Level of progesterone in ESR agonists medium. (D) Level of progesterone in ESR antagonists medium. (E) Level of testosterone in ESR agonists medium. (D) Level of testosterone in ESR antagonists medium. All experiments were performed in 2 replicates.

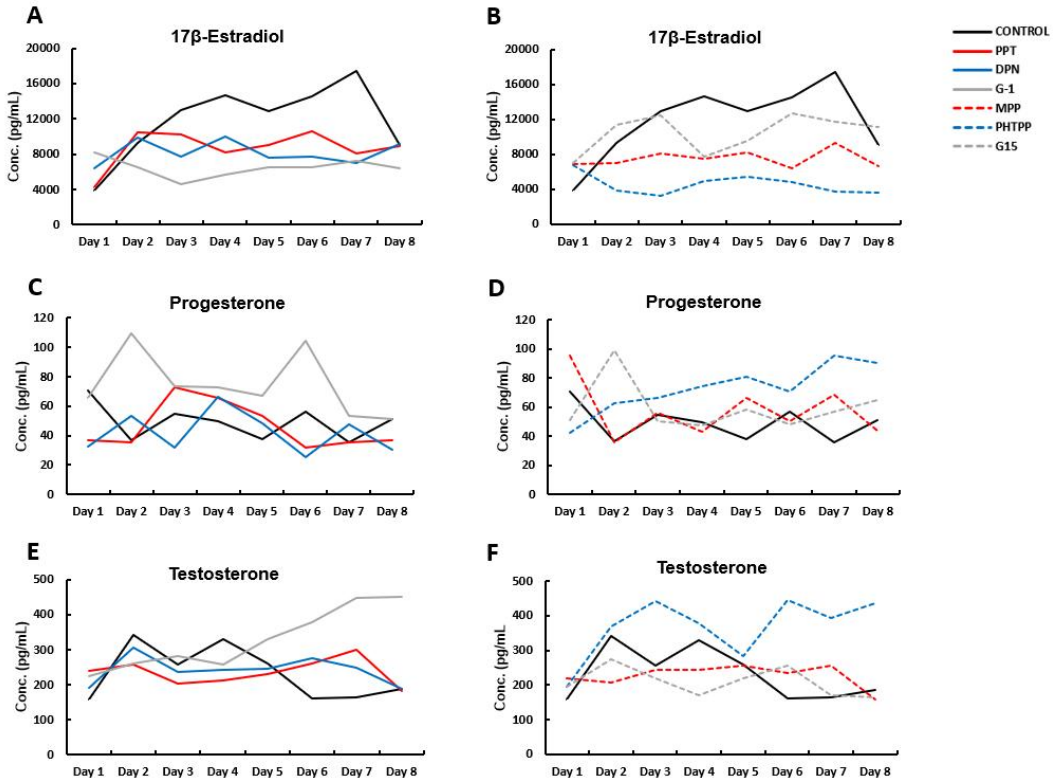

Figure 12. *in vitro* culture effect by estrogen receptor ago/antagonist on the steroid hormonal level of *Amh* -/- ovaries during the culture period.

Hormonal level was estimated in spent media by the ELISA kit. (A) Level of 17β-Estradiol in ESR agonists medium. (B) Level of 17β-Estradiol in ESR antagonists medium. (C) Level of progesterone in ESR agonists medium. (D) Level of progesterone in ESR antagonists medium. (E) Level of testosterone in ESR agonists medium. (D) Level of testosterone in ESR antagonists medium. All experiments were performed in 2 replicates.

DISCUSSION

In mammals, primordial follicles assembled in fetuses or during infancy constitute the oocyte resources for life. Exposure to 17 beta-estradiol and phytogenic of endocrine disrupting chemicals during pregnancy or perinatal period leads to the failure of normal follicle formation. When estradiol is injected to postnatal day 4 mouse ovary, nest breakdown is delayed and the percent of single oocyte is reduced. This result leads to an increase in unassembled follicles and a decrease the number of primordial follicles (Pepling et al, 2007). In chick ovary, E2 administration promote the primordial follicles transition to growing follicle through increasing ER and cadherins (Zha et al, 2017). Besides, it is also revealed that estrogen receptor 2 (ESR2) signaling is a keeper to block primordial follicle activation. Esr2 null rats result in increased activation of primordial follicle (Charkravarthi et al, 2020). On the other hand, AMH is well known regulator of follicle recruitment. However, the possible roles of estrogen and its receptors are still controverse and the relation between ERs and AMH is not known.

This study evaluated which estrogen receptor is critical in the process of primordial follicle activation. The localization patterns of ESR1, ESR2 and GPR30 did not change by whether follicles are a dormant or not in both wild type and *Amh* knockout mice. ESR1 and ESR2 were expressed in the oocyte cytoplasm, and GPR30 was expressed in the ooplasmal membrane. There was no difference in the degree of expression according to the genotype. In postnatal day 1, *Amh* knockout ovaries showed a reduced mRNA expression of all estrogen receptors and also protein expression decreased. Especially, the level of Esr1 was significantly low. As is known in previous studies that the *Amh* knockout group

is characterized to rapid depletion by recruiting more primordial follicles, the ratio of phosphorylation of mTOR and Akt1 was high. These are concerned with previous studies, estrogen receptor alpha, activated by estrogen, can bind to the 5′ region of the Amh gene and regulate transcription in ovaries cultured in basal medium (Tanimoto et al, 2021). An ERE is located in human AMH and the exogenous human AMH promoter can be activated by estrogen (Guerrier et al, 1990).

GSE179888 including postnatal day 0 to 14 *in vivo* ovaries total RNAseq dataset was reanalyzed and clustered the genes. by similar expression pattern of genes. Genes that up-and down-regulated at postnatal day 7 compared to day 0 were selected. Among the categories that up-regulated genes involved in, steroid metabolic process, and regulation of reproductive process-related genes showed a similar expression pattern in cultured ovary with *in vivo* samples. compared to fresh ovaries. Unexpectedly, genes in the meiosis Ⅰ category containing down-regulated genes had an increased level after culture in the wild type. *Amh* knockout group showed the same decrease as in vivo. Homeostasis related gene, Ank1, there was no significant difference in both groups but the decreasing tendency was the same. Those results show the in vitro culture is reasonable to study the activation of primordial follicles.

In vitro ovarian culture with each receptor's agonist and antagonist was performed. In all treatment groups, the *Amh* knockout ovaries had expectedly a greater degree of activation than the wild type. Interestingly, in wild type, MPP-treated ovaries that repress estrogen receptor alpha showed a significantly high ratio of primary follicles. And the number of primary follicles was reduced the most in PPT medium. The upregulated influence of MPP worked the same in *Amh* knockout ovary but that was not significant. PPT presented just a similar

level of activation to control group. Unlike the wild type mice, G-1 significantly inhibited the activation of primordial follicles the most in *Amh* knockout. In addition, there was no effect on agonist and antagonist on estrogen receptor beta in both the wild type and *Amh* knockout group.

As it grows into a primary follicle, the extracelluar matrix surrounding the follicle is digested. Cathepsin is a papain-like cysteine protease. The inhibitor of cathepsin, stefin, repressed the growth of primordial follicles in culture postnatal day 0 ovaries in a previous study (Komatsu et al, 2021). Additionally, there is an increase in the degree of collagen type IV digestion and the ratio of phosphorylation of Foxo3 in ovaries cultured by treatment with ICI 182,780, and estrogen receptor antagonist. It is known that estrogen can be also involved in ECM digestion around primordial follicles. As depicted in the result of transcriptomic analysis the ECM related genes are dramatically changed. Therefore, the digested pattern of ECM including collagen type IV and fibronectin will be additionally analyzed lby comparing the results of the different activation ratio in the chemical-treated culture results. And for another further study, in order to investigate the clear mechanism between AMH and ESR1, the *in vitro* culture will be performed with *Esr1* knockout mice and *Amh*, *Esr1* double knockout mice to compare the primordial follicle activation.

Put together, these results clearly showed that the mRNA and protein of ESR1 decreased in *Amh* knockout ovaries which exhibits premature follicle depletion phenotype. And cultured ovary in MPP to reduce ESR1 showed the proportion of primary follicles was the highest, but the dormant follicle was high in the PPT. In Amh knockout group, MPP and PPT did not have a significant role in activation and G-1 blocked activation. Therefore, AMH may involved in E2 mediates estrogen receptor alpha to inhibit the primordial follicle activation step.

And in the absence of AMH, estrogen receptor alpha does not function properly, GPR30 may work instead of it.

REFERENCES

Abdi S, Salehnia M, Hosseinkhani S. Steroid Production and Follicular Development of Neonatal Mouse Ovary during in vitro Culture. Int J Fertil Steril. 2013 Oct;7(3):181-6. Epub 2013 Sep 18. PMID: 24520484; PMCID: PMC3914497.

Adhikari D, Zheng W, Shen Y, Gorre N, Hämäläinen T, Cooney AJ, Huhtaniemi I, Lan ZJ, Liu K. Tsc/mTORC1 signaling in oocytes governs the quiescence and activation of primordial follicles. Hum Mol Genet. 2010 Feb 1;19(3):397-410. doi: 10.1093/hmg/ddp483. Epub 2009 Oct 20. PMID: 19843540; PMCID: PMC2798719.

Amoushahi M, Lykke-Hartmann K. Distinct Signaling Pathways Distinguish in vivo From in vitro Growth in Murine Ovarian Follicle Activation and Maturation. Front Cell Dev Biol. 2021 Jul 23;9:708076. doi: 10.3389/fcell.2021.708076. PMID: 34368158; PMCID: PMC8346253.

Burks DM, McCoy MR, Dutta S, Mark-Kappeler CJ, Hoyer PB, Pepling ME. Molecular analysis of the effects of steroid hormones on mouse meiotic prophase I progression. Reprod Biol Endocrinol. 2019 Dec 2;17(1):105. doi: 10.1186/s12958-019-0548-x. PMID: 31791345; PMCID: PMC6886186.

Chakravarthi VP, Ghosh S, Roby KF, Wolfe MW, Rumi MAK. A Gatekeeping Role of ESR2 to Maintain the Primordial Follicle Reserve. Endocrinology. 2020 Apr 1;161(4):bqaa037. doi: 10.1210/endocr/bqaa037. PMID: 32141511..

Chen Y, Jefferson WN, Newbold RR, Padilla-Banks E, Pepling ME. Estradiol, progesterone, and genistein inhibit oocyte nest breakdown and primordial

follicle assembly in the neonatal mouse ovary in vitro and in vivo. Endocrinology. 2007 Aug;148(8):3580-90. doi: 10.1210/en.2007-0088. Epub 2007 Apr 19. PMID: 17446182.

Chen Y, Breen K, Pepling ME. Estrogen can signal through multiple pathways to regulate oocyte cyst breakdown and primordial follicle assembly in the neonatal mouse ovary. J Endocrinol. 2009 Sep;202(3):407-17. doi: 10.1677/JOE-09-0109. Epub 2009 Jun 8. PMID: 19505948.

Devillers MM, Petit F, Cluzet V, François CM, Giton F, Garrel G, Cohen-Tannoudji J, Guigon CJ. FSH inhibits AMH to support ovarian estradiol synthesis in infantile mice. J Endocrinol. 2019 Feb 1;240(2):215-228. doi: 10.1530/JOE-18-0313. PMID: 30403655.

Durlinger AL, Gruijters MJ, Kramer P, Karels B, Ingraham HA, Nachtigal MW, Uilenbroek JT, Grootegoed JA, Themmen AP. Anti-Müllerian hormone inhibits initiation of primordial follicle growth in the mouse ovary. Endocrinology. 2002 Mar;143(3):1076-84. doi: 10.1210/endo.143.3.8691. PMID: 11861535.

Dutta S, Burks DM, Pepling ME. Arrest at the diplotene stage of meiotic prophase I is delayed by progesterone but is not required for primordial follicle formation in mice. Reprod Biol Endocrinol. 2016 Dec 5;14(1):82. doi: 10.1186/s12958-016-0218-1. PMID: 27919266; PMCID: PMC5139117.

Fuentes N, Silveyra P. Estrogen receptor signaling mechanisms. Adv Protein Chem Struct Biol. 2019;116:135-170. doi: 10.1016/bs.apcsb.2019.01.001. Epub 2019 Feb 4. PMID: 31036290; PMCID: PMC6533072.

Hardy K, Mora JM, Dunlop C, Carzaniga R, Franks S, Fenwick MA. Nuclear exclusion of SMAD2/3 in granulosa cells is associated with primordial follicle activation in the mouse ovary. J Cell Sci. 2018 Sep 7;131(17):jcs218123. doi: 10.1242/jcs.218123. PMID: 30111581.

Jefferson WN, Couse JF, Padilla-Banks E, Korach KS, Newbold RR. Neonatal exposure to genistein induces estrogen receptor (ER)alpha expression and multioocyte follicles in the maturing mouse ovary: evidence for ERbeta-mediated and nonestrogenic actions. Biol Reprod. 2002 Oct;67(4):1285-96. doi: 10.1095/biolreprod67.4.1285. PMID: 12297547.

John GB, Gallardo TD, Shirley LJ, Castrillon DH. Foxo3 is a PI3K-dependent molecular switch controlling the initiation of oocyte growth. Dev Biol. 2008 Sep 1;321(1):197-204. doi: 10.1016/j.ydbio.2008.06.017. Epub 2008 Jun 20. PMID: 18601916; PMCID: PMC2548299.

Kezele PR, Nilsson EE, Skinner MK. Insulin but not insulin-like growth factor-1 promotes the primordial to primary follicle transition. Mol Cell Endocrinol. 2002 Jun 28;192(1-2):37-43. doi: 10.1016/s0303-7207(02)00114-4. PMID: 12088865.

Kipp JL, Kilen SM, Bristol-Gould S, Woodruff TK, Mayo KE. Neonatal exposure to estrogens suppresses activin expression and signaling in the mouse ovary. Endocrinology. 2007 May;148(5):1968-76. doi: 10.1210/en.2006-1083. Epub 2007 Jan 25. PMID: 17255206.

Komatsu K, Wei W, Murase T, Masubuchi S. 17β-Estradiol and cathepsins control primordial follicle growth in mouse ovaries. Reproduction. 2021 Sep 6;162(4):277-287. doi: 10.1530/REP-20-0599. PMID: 34324431.

Lei L, Jin S, Mayo KE, Woodruff TK. The interactions between the stimulatory effect of follicle-stimulating hormone and the inhibitory effect of estrogen on mouse primordial folliculogenesis. Biol Reprod. 2010 Jan;82(1):13-22. doi: 10.1095/biolreprod.109.077404. Epub 2009 Jul 29. PMID: 19641178; PMCID: PMC2796699.

Liu L, Liu B, Li K, Wang C, Xie Y, Luo N, Wang L, Sun Y, Huang W, Cheng Z, Liu S. Identification of Biomarkers for Predicting Ovarian Reserve of Primordial Follicle via Transcriptomic Analysis. Front Genet. 2022 May 25;13:879974. doi: 10.3389/fgene.2022.879974. PMID: 35692832; PMCID: PMC9174591.

Mi X, Jiao W, Yang Y, Qin Y, Chen ZJ, Zhao S. HGF Secreted by Mesenchymal Stromal Cells Promotes Primordial Follicle Activation by Increasing the Activity of the PI3K-AKT Signaling Pathway. Stem Cell Rev Rep. 2022 Jun;18(5):1834-1850. doi: 10.1007/s12015-022-10335-x. Epub 2022 Jan 28. PMID: 35089464; PMCID: PMC9209380..

Mu X, Tu Z, Chen X, Hong Y, Geng Y, Zhang Y, Ji X, Liu T, Wang Y, He J. In utero Exposure to Excessive Estrogen Impairs Homologous Recombination and Oogenesis via Estrogen Receptor 2 in Mice. Front Cell Dev Biol. 2021 Jun 4;9:669732. doi: 10.3389/fcell.2021.669732. PMID: 34150762; PMCID: PMC8212019.

Myers M, Britt KL, Wreford NG, Ebling FJ, Kerr JB. Methods for quantifying follicular numbers within the mouse ovary. Reproduction. 2004 May;127(5):569-80. doi: 10.1530/rep.1.00095. PMID: 15129012.

Nilsson EE, Skinner MK. Growth and differentiation factor-9 stimulates progression of early primary but not primordial rat ovarian follicle

development. Biol Reprod. 2002 Sep;67(3):1018-24. doi: 10.1095/biolreprod.101.002527. PMID: 12193416..

Nilsson EE, Skinner MK. Kit ligand and basic fibroblast growth factor interactions in the induction of ovarian primordial to primary follicle transition. Mol Cell Endocrinol. 2004 Feb 12;214(1-2):19-25. doi: 10.1016/j.mce.2003.12.001. PMID: 15062541.

Nilsson EE, Kezele P, Skinner MK. Leukemia inhibitory factor (LIF) promotes the primordial to primary follicle transition in rat ovaries. Mol Cell Endocrinol. 2002 Feb 25;188(1-2):65-73. doi: 10.1016/s0303-7207(01)00746-8. PMID: 11911947.

Pelosi E, Omari S, Michel M, Ding J, Amano T, Forabosco A, Schlessinger D, Ottolenghi C. Constitutively active Foxo3 in oocytes preserves ovarian reserve in mice. Nat Commun. 2013;4:1843. doi: 10.1038/ncomms2861. PMID: 23673628; PMCID: PMC4504230.

Ren Y, Suzuki H, Jagarlamudi K, Golnoski K, McGuire M, Lopes R, Pachnis V, Rajkovic A. Lhx8 regulates primordial follicle activation and postnatal folliculogenesis. BMC Biol. 2015 Jun 16;13:39. doi: 10.1186/s12915-015-0151-3. PMID: 26076587; PMCID: PMC4487509.

Tanimoto R, Sekii K, Morohaku K, Li J, Pépin D, Obata Y. Blocking estrogen-induced AMH expression is crucial for normal follicle formation. Development. 2021 Mar 19;148(6):dev197459. doi: 10.1242/dev.197459. PMID: 33658225; PMCID: PMC7990856.

Tarumi W, Itoh MT, Suzuki N. Effects of 5α-dihydrotestosterone and 17β-estradiol on the mouse ovarian follicle development and oocyte maturation.

PLoS One. 2014 Jun 9;9(6):e99423. doi: 10.1371/journal.pone.0099423. PMID: 24911314; PMCID: PMC4050053.

Terren C, Nisolle M, Munaut C. Pharmacological inhibition of the PI3K/PTEN/Akt and mTOR signalling pathways limits follicle activation induced by ovarian cryopreservation and in vitro culture. J Ovarian Res. 2021 Jul 19;14(1):95. doi: 10.1186/s13048-021-00846-5. PMID: 34275490; PMCID: PMC8287691.

Vitt UA, McGee EA, Hayashi M, Hsueh AJ. In vivo treatment with GDF-9 stimulates primordial and primary follicle progression and theca cell marker CYP17 in ovaries of immature rats. Endocrinology. 2000 Oct;141(10):3814-20. doi: 10.1210/endo.141.10.7732. PMID: 11014238.

Wang C, Prossnitz ER, Roy SK. Expression of G protein-coupled receptor 30 in the hamster ovary: differential regulation by gonadotropins and steroid hormones. Endocrinology. 2007 Oct;148(10):4853-64. doi: 10.1210/en.2007-0727. Epub 2007 Jul 19. PMID: 17640985.

Wang C, Prossnitz ER, Roy SK. G protein-coupled receptor 30 expression is required for estrogen stimulation of primordial follicle formation in the hamster ovary. Endocrinology. 2008 Sep;149(9):4452-61. doi: 10.1210/en.2008-0441. Epub 2008 May 22. PMID: 18499747; PMCID: PMC2553386.

Wang Y, Teng Z, Li G, Mu X, Wang Z, Feng L, Niu W, Huang K, Xiang X, Wang C, Zhang H, Xia G. Cyclic AMP in oocytes controls meiotic prophase I and primordial folliculogenesis in the perinatal mouse ovary. Development. 2015 Jan 15;142(2):343-51. doi: 10.1242/dev.112755. Epub 2014 Dec 11. PMID: 25503411.

Wei W, Komatsu K, Osuka S, Murase T, Bayasula B, Nakanishi N, Nakamura T, Goto M, Iwase A, Masubuchi S, Kajiyama H. Tamoxifen Activates Dormant Primordial Follicles in Mouse Ovaries. Reprod Sci. 2022 Dec;29(12):3404-3412. doi: 10.1007/s43032-022-00896-0. Epub 2022 Feb 25. PMID: 35212933; PMCID: PMC9734234.

Yan H, Zhang J, Wen J, Wang Y, Niu W, Teng Z, Zhao T, Dai Y, Zhang Y, Wang C, Qin Y, Xia G, Zhang H. CDC42 controls the activation of primordial follicles by regulating PI3K signaling in mouse oocytes. BMC Biol. 2018 Jul 5;16(1):73. doi: 10.1186/s12915-018-0541-4. PMID: 29976179; PMCID: PMC6033292.

Yan H, Wen J, Zhang T, Zheng W, He M, Huang K, Guo Q, Chen Q, Yang Y, Deng G, Xu J, Wei Z, Zhang H, Xia G, Wang C. Oocyte-derived E-cadherin acts as a multiple functional factor maintaining the primordial follicle pool in mice. Cell Death Dis. 2019 Feb 15;10(3):160. doi: 10.1038/s41419-018-1208-3. PMID: 30770786; PMCID: PMC6377673.

Zhang H, Risal S, Gorre N, Busayavalasa K, Li X, Shen Y, Bosbach B, Brännström M, Liu K. Somatic cells initiate primordial follicle activation and govern the development of dormant oocytes in mice. Curr Biol. 2014 Nov 3;24(21):2501-8. doi: 10.1016/j.cub.2014.09.023. Epub 2014 Oct 23. PMID: 25438940.

Zhang T, He M, Zhao L, Qin S, Zhu Z, Du X, Zhou B, Yang Y, Liu X, Xia G, Chen T, Wang Y, Zhang H, Wang C. HDAC6 regulates primordial follicle activation through mTOR signaling pathway. Cell Death Dis. 2021 May 29;12(6):559. doi: 10.1038/s41419-021-03842-1. PMID: 34052832; PMCID: PMC8164630.

Zhang X, Liu G, Zhang N, Hua K. A time-resolved transcriptome landscape of the developing mouse ovary. Biochem Biophys Res Commun. 2021 Oct 1;572:57-64. doi: 10.1016/j.bbrc.2021.07.083. Epub 2021 Jul 31. PMID: 34343835.

Zhao Y, Feng H, Zhang Y, Zhang JV, Wang X, Liu D, Wang T, Li RHW, Ng EHY, Yeung WSB, Rodriguez-Wallberg KA, Liu K. Current Understandings of Core Pathways for the Activation of Mammalian Primordial Follicles. Cells. 2021 Jun 13;10(6):1491. doi: 10.3390/cells10061491. PMID: 34199299; PMCID: PMC8231864.

Zhao D, Lv C, Liu G, Mi Y, Zhang C. Effect of estrogen on chick primordial follicle development and activation. Cell Biol Int. 2017 Jun;41(6):630-638. doi: 10.1002/cbin.10766. Epub 2017 Apr 11. PMID: 28328180.

논문개요

증가된 원시 난포 활성화는 난소에 남아있는 난포의 빠른 고갈과 조기 난소 기능 부전을 유도하므로 원시 난포 활성화의 조절은 가임력 보존에 있어 중요한 단계 중 하나다. 스테로이드 호르몬, 특히 에스트로겐은 초기 난포 형성 및 발달과 관련하여 중요한 역할을 하는 것으로 알려져 있다. 많은 연구에서 원시 난포 활성화와 에스트로겐 농도 사이의 관계가 예측되어 왔지만, 그 수용체와 관련하여 가장 관련있는 기작에 대해 연구된 바가 없다. 본 연구에서는 항-뮐러 호르몬(Amh) 녹아웃 생쥐와 체외 배양 시스템을 사용하여 에스트로겐 수용체 각각에 대한 작용제와 길항제를 처리했을 때 원시 난포 활성화 정도를 비교하였다. ESR1 과 ESR2 는 휴면 및 활성 난포의 세포질에 국소화되었다. Esr1 mRNA 와 단백질의 발현 수준은 *Amh* 녹아웃 난소에서 유의하게 낮았지만 Esr2 와 Gper1 은 그렇지 않았다. 예상대로 인산화된 mTOR 과 Akt1 의 비율이 *Amh* KO 생쥐의 난소에서 높았다. 체내 유전자의 발현 패턴을 분석하여 군집화하고 체외배양 결과에 도입해 분석하였다. 야생형 생쥐의 난소에서 ESR1 길항제인 MPP 처리된 그룹이 가장 높은 원시 난포 활성화 정도를 보였고 휴면 난포는 ESR1 작용제인 PPT 처리군에서 많게 나타났다. 반면 *Amh* 녹아웃 난소에서 MPP 와 PPT 는 유의적인 영향을 미치지 않고 대신 GPR30 작용제인 G-1 이 활성화를 억제하는 효과를 보였다. 따라서 AMH 는 에스트로겐을 매개하여 원시 난포 활성화를 억제할 수 있다. 그리고 AMH 가 작용하지 못할 때, ESR1 이 제대로 기능하지 않으면 GPR30 이 대신 작동할 수 있다. 이러한 결과는 원시 난포 활성화에 ESR1 이 중요한 역할을 하고 있음을 시사하며 추가 연구로 *Esr1* 단독 녹아웃 및 *Esr1*, *Amh* 이중 녹아웃 생쥐 난소를 체외배양하여 원시 난포 활성화 정도를 비교할 필요가 있다. 또한 원시 난포가 성장함에 따라 난포 주변을 둘러싸고 있는 세포외기질이 분해되므로, 체외배양했을 때 세포외기질의 변화 패턴도 추가적으로 분석하고자 한다.